

NONAPPLICABILITY OF
LINEAR FINITE ELEMENT PROGRAMS TO THE
STRESS ANALYSIS OF TIRES

by Michel Durand and Etienne Jankovich

KLEBER-COLOMBES, Theoretical Tire Engineering,
COLOMBES, France

SUMMARY

A static finite element stress analysis of an inflated radial car tire is carried out. The deformed shape of the sidewall presents an outward bulging. The analysis of a homogeneous isotropic toroidal shell shows that the problem is common to all solids of this type. The study suggests that the geometric stiffness due to the inflation pressure has to be taken into account. Also, the resulting large displacements make it necessary for the geometry to be up-dated at each load step.

16

INTRODUCTION

The tire is a mass-produced industrial product, and therefore those who are not specialists tend to believe that its mechanical behavior is well known and precisely analyzed. However, the tire engineer knows that this is not the case because of the rather unique characteristics of rubber.

A survey of available literature shows that most often empirical methods are used to determine the behavior of existing tires (References 1, 2 and 3). In the design field a few analytical methods are available to determine the dimensional and inflated geometry of the tire (References 4, 5 and 6). In addition, results of wider applicability have been obtained by Zorowski using finite element shell theory type modelization which included nonlinear relations of the mid-surface strain (Reference 7).

The reasons for the lack of theoretical work are that stress analysis of tires is a rather formidable task. It involves large displacement analysis, nearly incompressible materials, viscoelasticity and thermal conduction and radiation. At the same time one must account for the heat generated under dynamic loading conditions. Heretofore it has not been possible to solve even part of the problem by the most powerful analytical methods. Recently, however, large-size finite element methods became available and were applied successfully to a number of complex problems. Because of the generality of these programs, it was thought that the method might be applicable to stress analysis of tires.

The ASKA program was selected because it has a very wide variety of finite elements which includes tridimensional elements. Some other programs, such as TITUS, developed in France by CITRA, have also been tested. However, the most significant results were obtained by means of ASKA. A singular point is encountered on the sidewall of the tire. Different solutions are proposed and their economical feasibility are discussed.

SYMBOLS

u displacement , m
 σ stress , MN/m²
Subscript:
R, Z and T radial, axial, and hoop components

ANALYSIS OF THE TIRE

The calculations were carried out on a radial type KLEBER V10 RS experimental Rallye-Racing tire. A cross-sectional view of the initial shape taken as the mold shape of the tire is shown in Figure 1. The bead wires are made of steel and the flipper is a nylon fabric with the fibers lying at $\pm \pi/4$ rad relative to the radius. The carcass is made of textile with fibers having a radial orientation. The belt has four layers of glass-fiber cords supplied by OWENS CORNING FIBERGLASS forming an angle of ± 0.35 rad with the equatorial plan. The tube-type tire is fitted on a 7 J 13 rim. In the course of determining the material properties, several problems had to be solved.

1 - Rubber - Experimentally it has been established that for deformations not exceeding 10-15 % mm/mm, the usual HOOKE law applies to vulcanizates. The HOOKE's coefficients are determined making allowance for the instantaneous geometry of the specimen (Reference 8). For all rubber elements, the assumed POISSON's ratio is 0.49. Tests were carried out on normalized flat uniaxial tensile test pieces cut out of the vulcanized tire.

2 - Composite Materials - The strains in composite specimens were determined by taking photographs: one before and one after deformation. A network of orthogonal lines drawn on the surface of the specimen was used as a benchmark. The aim was to investigate the material properties at low strains in the range which obeys the HOOKE's law (Reference 9).

Finite element idealization

The ASKA program, 4.2 Level, was selected to calculate the static stresses in the tire. The inflated tire was analyzed with the help of TRIAX 6 and TRIAXC 6 linearly varying strain ring elements. The index C is relative to a curved-edge element. Both elements can be anisotropic, have six nodes, and support only axisymmetric loads. Each node has two displacement degrees of freedom.

The idealization shown Figure 2 encompasses about 577 elements and 1300 nodes. All elements have a ratio of the smaller edge to the larger one that is at least equal to 1/7. However, in some places, such as the bead wires, the angle of two edges was much smaller than $\pi/3$ rad.

a - Tread - Half the thickness of the tire's tread was removed. In this case, the tread grooves can be assumed to be axisymmetric, and a more realistic tread groove cracking analysis can be carried out. The material is assumed to be isotropic.

b - Belt - It is idealized by means of an orthotropic equivalent material. The generalized HOOKE's coefficients are determined using coefficients obtained by single-layer tests and the equations in Reference 10.

c - Rubber reinforcement at the edge of the belt - gum tip - isotropic.

d - The carcass is orthotropic. No provisions were made for making allowance for shaping the carcass before vulcanization. HOOKE's coefficients are determined as for the belt.

e - Sidewall - isotropic

f - Rim load transfer rubber - rim cushion - isotropic.

g - Bead filler - isotropic

h - Flipper - Idealized by means of an equivalent orthotropic material using the corrected equations in Reference 10 (page 77).

i - Bead wires are analyzed like the flipper. The equivalent material is orthotropic.

j - Inner liner - isotropic.

l - Boundary conditions - In the equatorial plane all u_z have been assumed to equal zero. The influence of the rim has been taken into account by

assuming that the rim is rigid and that the tire takes the form of the rim along the contact area.

One possibility is that the exact contact area may be determined by observing the sign of the normal contact stresses and modifying by trial and error the assumed boundary displacements.

2 - Loading cases - In the first case it was assumed that there was a pressure of 0.1 MN/m² and zero displacement within the initial rim contact area. The second case was the study at zero inflation pressure of the effect of mounting the tire on the rim. In the third case the two preceding cases are combined assuming an inflation pressure of 0.25 MN/m².

RESULTS

A verification of the input data was carried out by in-house plotting packages. A program, for instance, involves plotting the contour of each particular material. It is also possible to plot the mesh showing either the contour of each element or the location of the nodes. Any element that is missing appears as an inlet in the contour line of the material.

To obtain an image of the stress, ASKA gives only the elemental stresses of anisotropic materials. Thus, it was necessary to set up a program to determine the arithmetic mean for each material separately. Standard deviation was also determined. Stress contours were plotted for the σ_{RR} , σ_{ZZ} , σ_{TT} and σ_{RZ} . Because the stress distribution is linear across an element, the contours cross the elements in straight-line segments. Thus, the adequacy of the mesh can be assessed. The results obtained are shown in Figures 4 and 5.

There are two ways to use the information given by the stress contours. In the part of the tire where the behavior is linear, the results can be used to analyze the tire quantitatively and to predict its fatigue behavior. In the range where the behavior is nonlinear, the results can be used for a qualitative assessment of the fatigue performance of the particular detail. In this case, the magnitude of the stress concentration rather than the gross stresses are obtained. The stress concentrations are located in ranges where fatigue problems have been actually encountered.

It may be of interest to the designer to know that inflated tire results can already indicate where fatigue problems occur during the service life of the tire. For example, cracks tend to grow along the length of the groove which is next to the shoulder. However, since the abrasion of a racing tire is very rapid, there is not enough time for any cracks to grow. Figure 4 shows that at the tread groove location the highest positive stress is σ_{ZZ} . Cracks are generally produced normal to the largest tension stress. Furthermore, none of the other grooves have a large stress concentration. Thus, both the orientation of the crack and its location can be predicted by

a finite element stress analysis. Because of the low modulus of the rubber, it is to be noted that the strains at the shoulder groove are about 20 % mm/mm.

Another interesting result concerns the inner liner. The analysis shows that the inner liner has no effect on the deformation of the tire. Thus, to reduce the computation time the inner liner and, more generally, all non-load-carrying parts can be analyzed separately by applying to their boundary the displacements obtained in a preliminary calculation of the load-carrying elements of the tire.

CORRELATION OF TEST AND ASKA RESULTS

Figure 3 shows a plot of the deformed and initial geometry of the tire. On the sidewall, due to small bending stiffness and the large displacements occurring in this part, the tire bulges outward. Further, the deformed tire has a point of inflection that has never been observed on a tire.

An experimental check was carried out by measuring the tire's circumference and its maximum section width. The solid-line curve shows the theoretical results and the triangles show the test points. (See Figures 6-9). At a pressure as high as the service pressure of 0.25 MN/m², agreement between theory and tests is satisfactory on the center line of the tread and the adjacent area (Figures 6 and 7). However, as shown by Figures 8 and 9, outside this range the computed displacements do not agree with the measured ones. Notice that the tire width change is a nonlinear function of the pressure starting from pressures as low as 0.03 MN/m².

TOROIDAL SIDEWALL SINGULARITY

The problem of the sidewall singularity in the tire is a part of the very complex tire problem.

It was therefore decided to study a similar but much simpler solid such as a toroidal isotropic shell. The cross-section of the toroidal shell was circular, its thickness was 10^{-3} m, its YOUNG's modulus was 2.5 MN/m² and its POISSON's ratio was 0.49. It was inflated to .0074 MN/m². Figure 10 shows the initial and deformed geometry obtained by means of TRIAX 6 elements. The same type of behavior as previously observed in the tire occurs again.

Experiments are described in Reference 11 showing the deformed shape of the solid described above. A nearly perfect circular cross section was found. Thus, the bulging of the sidewall is a purely mathematical problem. At the singularity point, one radius of curvature becomes infinite. The problem is similar to that of a transversely loaded clamped membrane plate. The equili-

brium of the forces can only be obtained by taking into account the deformed surface of the membrane. In finite element analysis, however, due to the fact that curves are approximated by straight lines, the chance of obtaining an infinite radius of curvature is very slight.

The explanation for the singularity that is nevertheless observed was given in Reference 12. It was established in the above reference paper that the sidewall singularity of the membrane toroid is not removed by introducing the bending stiffness. The pressurized shell has a pressure stiffness in addition to its bending stiffness. Additional computations are carried out presently using small load step increments and up-dating the geometry following a load step. In this case, the singularity is attenuated. But the computation time increases linearly with the number of load steps chosen. The computation of one load step on CDC 6600/single precision, 3 substructures, 3 load cases, with 2 tapes takes 374 s CP, 1721 s PP and a field length of 47 K CM, for the TRIAX 6 modelization of the tire.

In the preceding discussion only linear finite element programs have been considered. However, programs with nonlinear capability are available.

In fact, several examples given at the NASTRAN Users' Colloquium show that NASTRAN's differential stiffness capability might offer more adequate means for solving the problem. Because of the lack of three-dimensional elements such a calculation could not be carried out until recently.

CONCLUSION

Linear finite element codes are not applicable to the analysis of toroidal solids because of the toroidal singularity. The geometric stiffness due to the inflation pressure must be taken into account. This can be done, for instance, by increasing the load step by step and up-dating the geometry.

Research is being carried out at the present time by KLEBER with the aim of developing or identifying finite element methods incorporating the above-described modifications to the classical equations.

In conclusion, the straight-forward stress analysis by means of available linear finite element programs is uneconomical, in any event, as long as the computation time cannot be reduced.

ACKNOWLEDGMENTS

The authors wish to express their appreciation to the Civil Engineering Section of the Société Informatique Appliquée, Metra International, and especially to their chief engineer, Mr. G. CANEVET, for their helpful advice concerning ASKA.

REFERENCES

1. CLARK, S.K., DODGE, R.N., LACKEY J.I. and NYBAKKEN, G.H., Structural Modeling of Aircraft Tires, University of Michigan, College of Engineering, Dept. of Mechanical Engineering, Technical Report No. 10, 05608-16-T, May 1970.
2. FRANK, F. and HOFFERBERTH, W., Mechanics of the Pneumatic Tire, Rubber Chemistry and Technology, Vol. 40, No. 1, February 1967, pp 271-322.
3. KERN, W.F., Verformungs- und Spannungsmessungen an Gürtelreifen, Kautschuk und Gummi-Kunststoffe, 24. Jahrgang, Nr. 11/1971, pp 599-608; 24. Jahrgang, Nr. 12/1971, pp 666-669.
4. CLARK, S.K., BUDD, C.B. and TIELKING, J.T., Tire Shape Calculations by the Energy Method, 1971 Congress of the West German Rubber Society (DKG), Wiesbaden, May 17-19, 1971.
5. BARSON, C.W., Mathematics of Modelling of Tire Performance, Akron Rubber Group's 1971 Spring Meeting, Akron, 1971.
6. ZOROWSKI, C.F. and DUNN, S.E., A Mathematical Model for the Pneumatic Tire, Report to Office of Vehicle Systems Research National Bureau of Standards, 1970.
7. ZOROWSKI, C.F., Mathematical Prediction of Dynamic Tire Behavior, Akron Rubber Group's 1971 Spring Meeting, Akron, 1971.
8. KUCHERSKII, A.M., Deformation Properties of Certain Vulcanisates at Low Deformations, Soviet Rubber Technology, March 1969, pp 27-29.
9. ZOLUTUKHINA, L.I. and LEPETOV, V.A., The Elastic Moduli of Flat Rubber - Fabric Constructions in Elongation and Compression, Soviet Rubber Technology, October 1968, pp 42-44.
10. ASHTON, J.E., HALPIN, J.C. and PETIT, P.H., Primer on Composite Materials : Analysis, Technomic Publication, Technomic Publishing Co., Inc., Stamford, Conn., 1969.
11. MERCIER, J., FREMAU, J. and ROCHA, A., Large Deformations and Stresses of a Thin, Highly Elastic, Toroidal Shell under Internal Pressure, Int. J. Solids Structures, 1970, Vol. 6, pp 1233-1241.
12. JORDAN, P.F., Analytical and Experimental Investigation of Pressurized Toroidal Shells, NASA CR-261, July 1965.

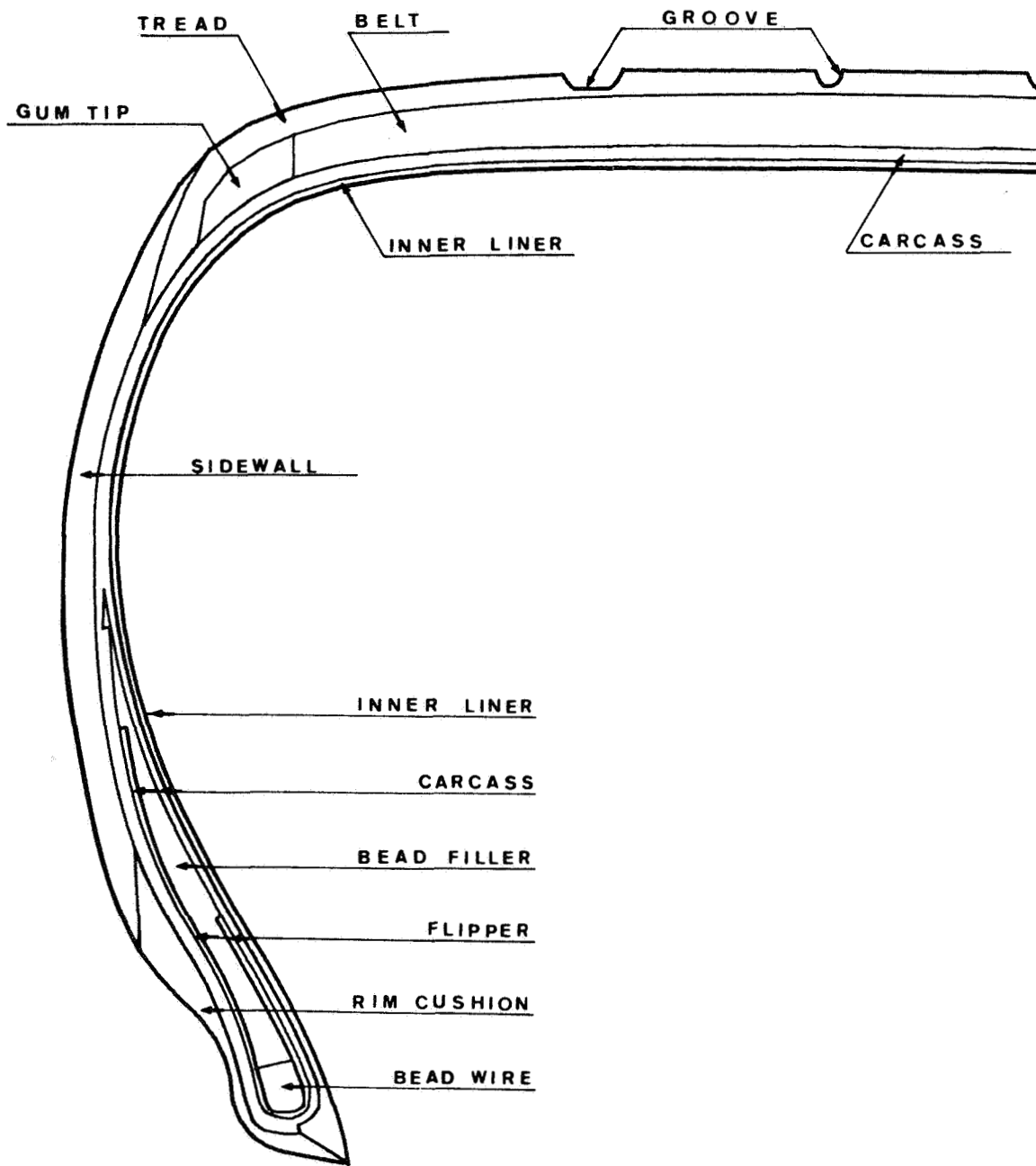


FIG. 1

**CROSS SECTION OF THE TIRE
KLEBER V 10 RS 210/55-13**

Scale 1. 4/1

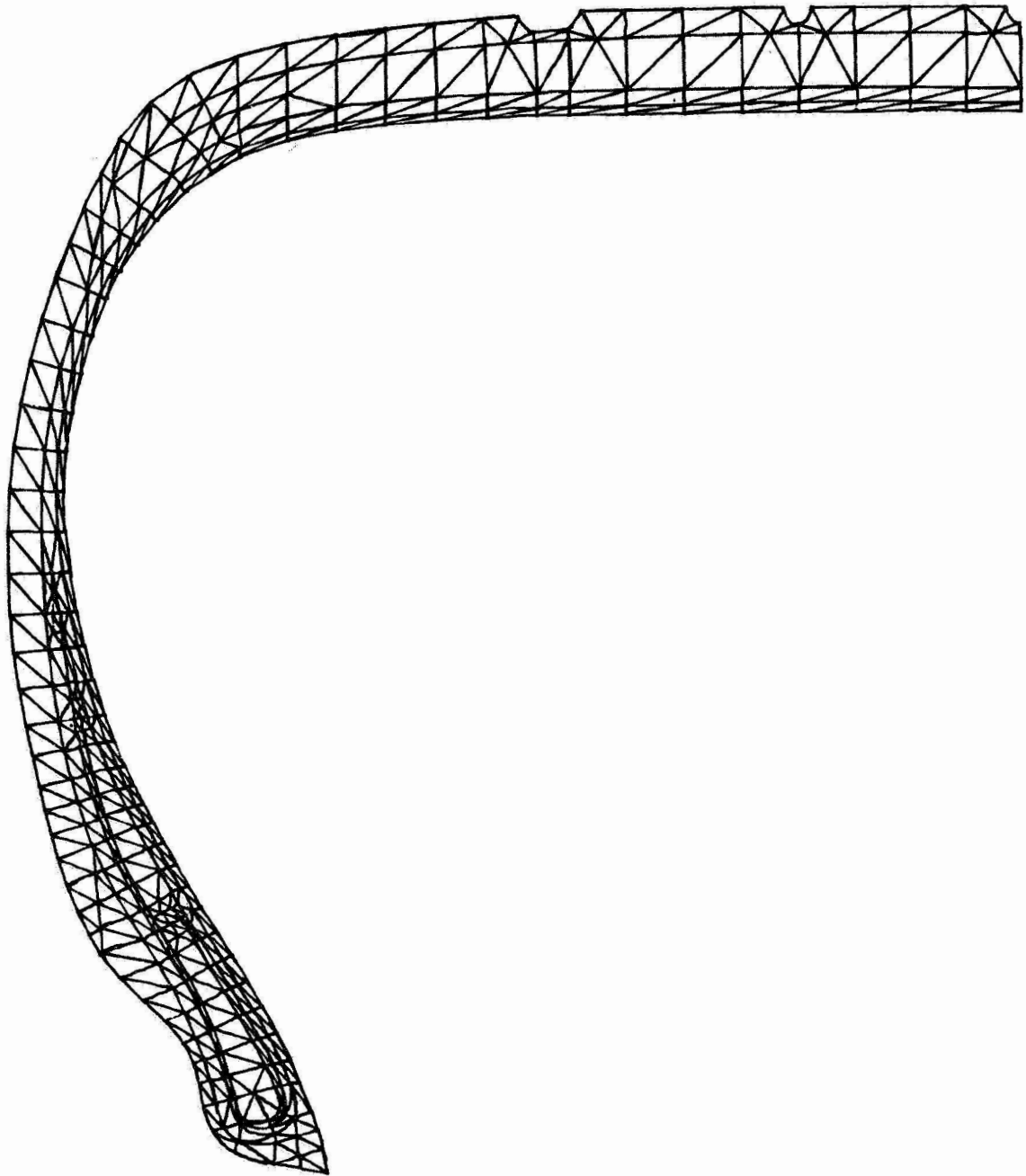


FIG. 2 **AXISYMMETRIC FINITE ELEMENT MODEL OF TIRE**

Scale 1.4/1

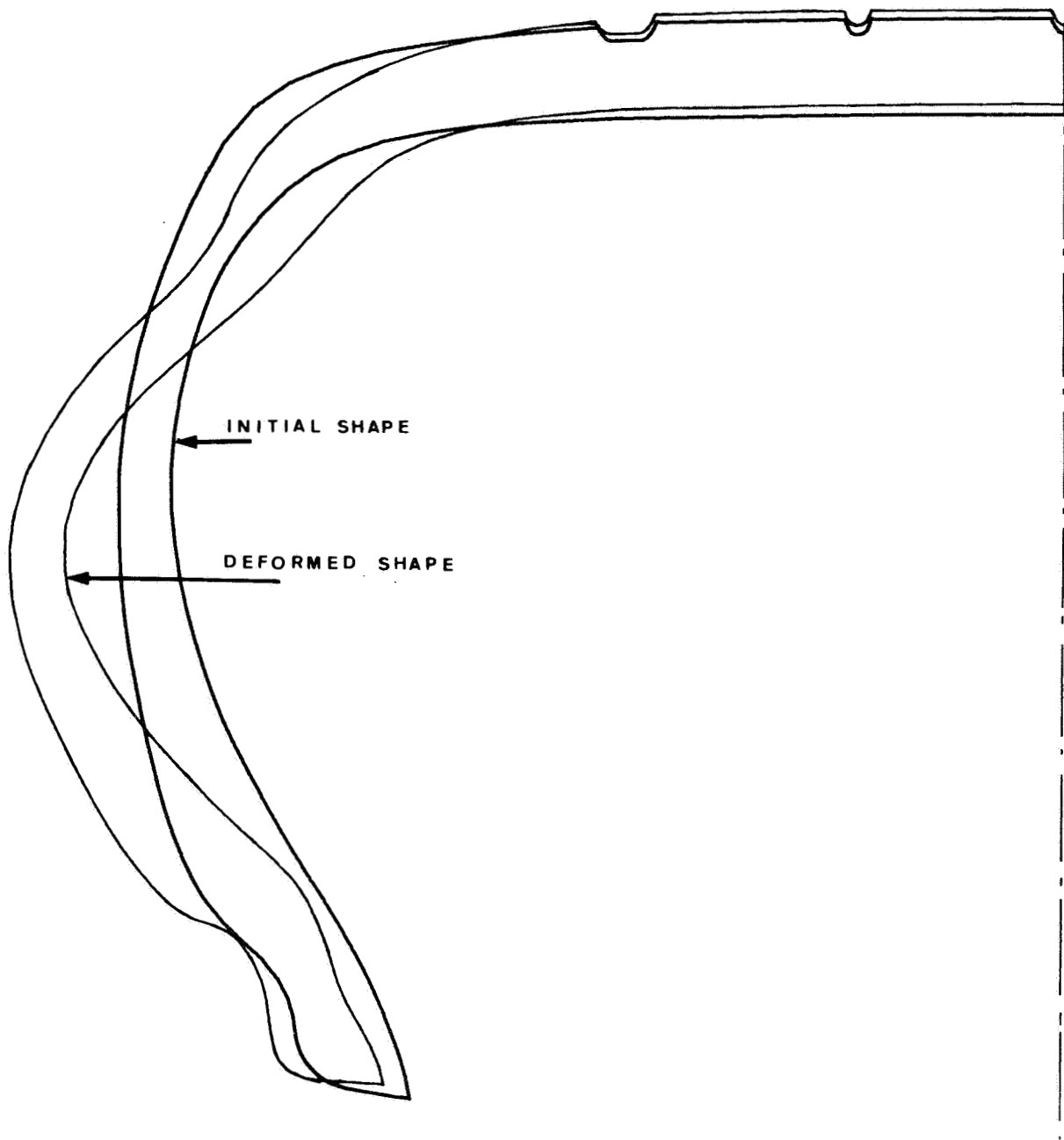


FIG. 3 **INITIAL AND DEFORMED SHAPE**

Loading case : inflation pressure 0.25 MN/m^2 and rim 7 J 13

Scale 1.4/1

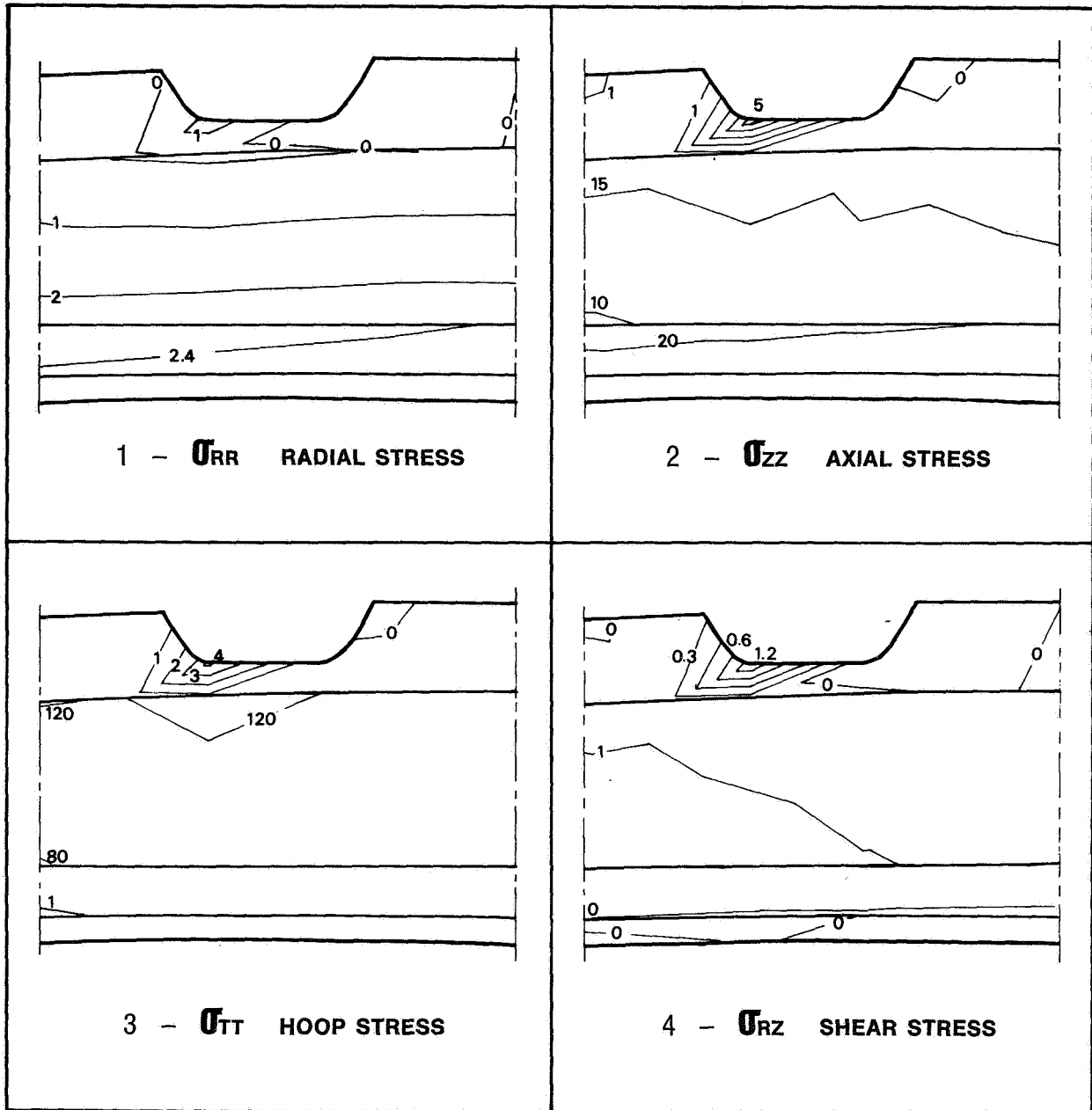
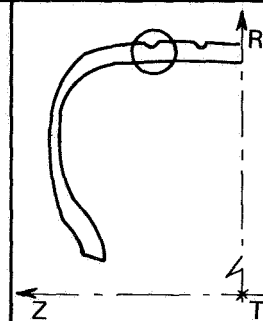


FIG. 4 STRESS CONTOURS AROUND THE GROOVE

Loading case : inflation pressure 0.25 MN/m^2
and rim 7 J 13

Scale 5/1

Stress unit : 0.1 MN/m^2



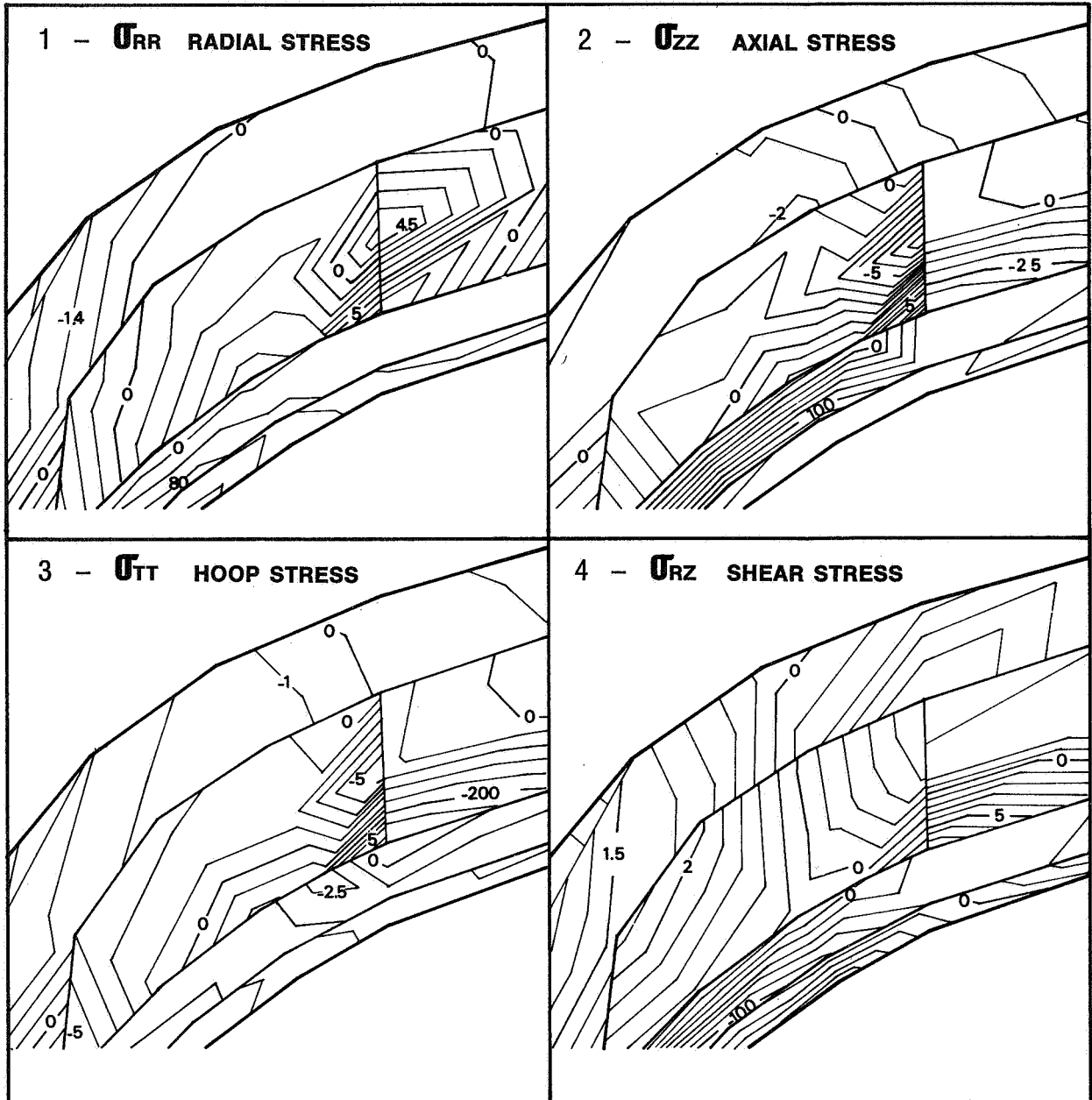
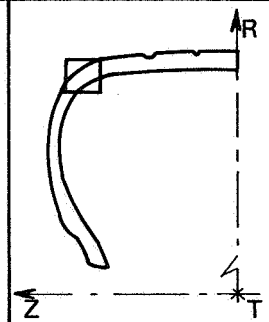


FIG. 5 STRESS CONTOURS AT THE BELT EDGE

Loading case : inflation pressure 0.25 MN/m²
and rim 7 J 13

Scale 5/1

Stress unit : 0.1 MN/m²



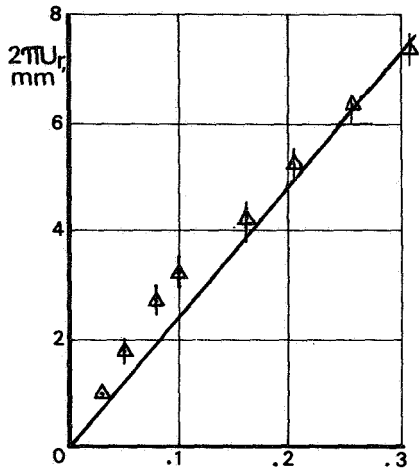


FIG. 6 Pressure, MN/m²

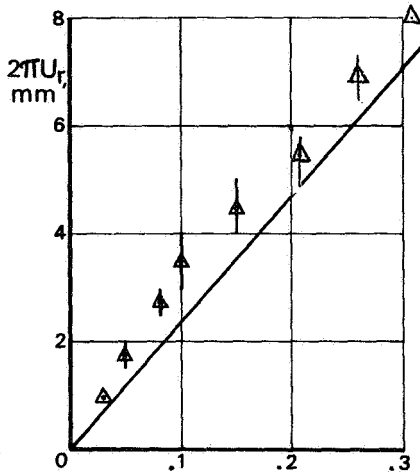


FIG. 7 Pressure, MN/m²

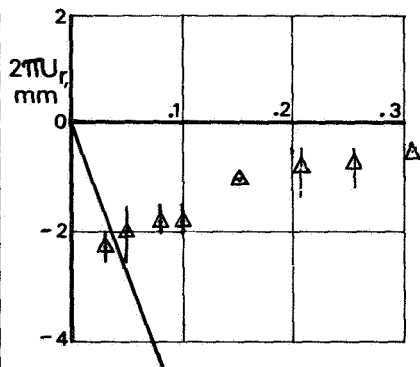
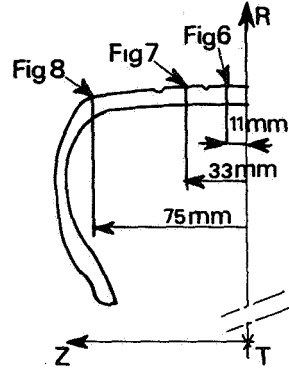


FIG. 8 Pressure, MN/m²

RADIAL DISPLACEMENT VS. INFLATION PRESSURE



△ Experiment - mean of 2 parallels
 - ASKA

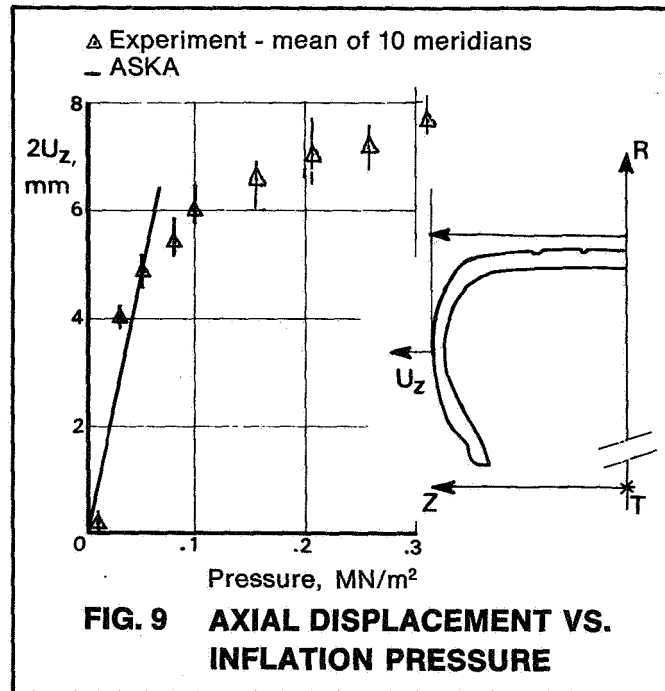


FIG. 9 AXIAL DISPLACEMENT VS. INFLATION PRESSURE

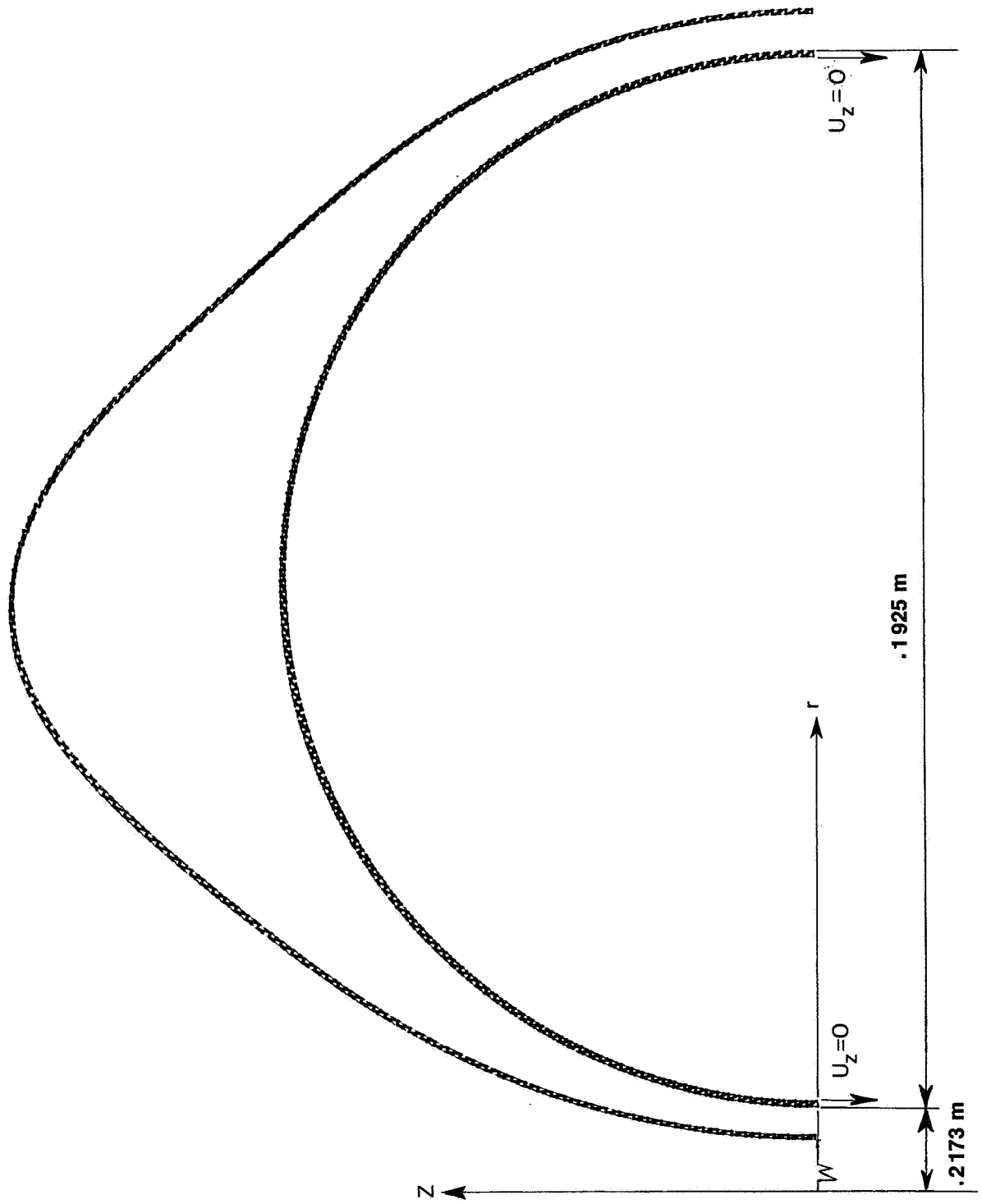


FIG. 10

TRIAx 6 MODEL OF TOROIDAL SHELL